Korean J. Chem. Eng., **22**(4), 512-520 (2005)

Molecular Dynamics Simulation Study of the Effect of PMMA Tacticity on Free Volume Morphology in Membranes

Kun-Tsung Lu and Kuo-Lun Tung†

Dept. of Chem. Eng. and R&D Center of Membrane Technology, Chung Yuan Christian University, Chung-Li, Taoyuan 320, Taiwan
(*Received 17 January 2005 • accepted 19 April 2005*)

Abstract–The effect of the tacticity of poly methyl methacrylate (PMMA) on the morphology of free volume in PMMA membranes was studied by using a molecular dynamics simulation technique. The chain flexibility, chain interaction, end-to-end distance of a chain and the time course of the free volume variation in the various stereo-regular PMMA, were obtained by an MD simulation technique. Simulation results depict that the construction of distinct tacticity has a significant influence on the flexibility of a molecular chain and the morphology of free volume in the syndiotactic (s-) and isotactic (i-) PMMA oligomers. MD calculation of the dynamic microstructure of a PMMA matrix shows that the s-PMMA membrane gives less flexibility in the backbone and a longer end-to-end distance than in the i-PMMA membrane. The less flexibility and longer end-to-end distance in the s-PMMA matrix causes the shapes and sizes of s-PMMA free volume to be longer and larger than those in an i-PMMA membrane. Furthermore, by adopting conformation energy minimization and molecular dynamics simulation techniques, various tacticity models of PMMA were constructed and their effect on the size of accessible free volume and free volume morphology was analyzed. Finally, the adsorbed gas on the surface free volume in s-PMMA was also compared with i-PMMA membrane.

Key words: Accessible Free Volume, Free Volume Morphology, *pcff* Force Field, PMMA Membrane, Tacticity

INTRODUCTION

Membrane-based gas separation processes have entered territories that were previously dominated by traditional unit operations such as for nitrogen/oxygen enriched air, natural gas treatment and/or hydrogen separation. The polymeric membranes for gas separation can be comprised from a variety of polymers, such as polyimide, polysulfone, polysiloxane, poly ether-ether-ketone, or poly methyl methacrylate etc. In the past two decades, some of the research efforts on the development of polymeric membrane for gas separation have been focused on the conformations of polymeric chains and related interactions of the matrix. For instance, stereo-regular conformation of polymeric membranes has been regarded to be one of the predominant factors affecting the membrane permeability.

Researches on the tacticity of PMMA can be divided into two categories: experimental and simulation approaches. In the former area, the main issues are the syntheses of stereo-regular membranes [Vorenkamp et al., 1979; Schroeder et al., 1985; Min and Paul, 1988], vibrational spectra of stereo-regular PMMA [Dybal et al., 1983; Kuebler et al., 1997], and differences of stereo-structure on glass transition temperature properties [Bywater and Toporowski, 1972; Grohens et al., 1998]. In the later studies, predictive spectrum [Koinuma et al., 1982], conformational statistics [Vacatello and Flory, 1986], and local dynamics of stereo-structure [Soldera and Grohens, 2002] have been conducted. Recently, it was pointed out that the applicable and successful development of theory and high-performance computing [Dongarra et al., 2001] on molecular simulation enabled the matrix interaction study to be carried out by the molecular dynamics simulation technique. MD simulation includes both Molecular Mechanics (MM) and Quantum Mechanics (QM) league. The molecular mechanics suitable for the membrane structure simulation is attributed to the lack of chemical reactions and lower calculating cost [Goodman, 1997; MacElroy, 2000].

The size distribution and its morphology of free volume in separation membranes were very important parameters for the polymeric membrane performance. Traditionally, there are experimental methods utilized to measure the size distribution and characterize the morphology of pore size in filtration and separation, include gas permeability, mercury porosimetry, and gas-liquid equilibrium methods [Mietton-Peuchot et al., 1997; Cuperus et al., 1992]. Hofmann et al. [2002] used a novel algorithm V_connect and R_max for analyzing the free volume size and its distribution. However, the morphology of free volume is still not fully understood. Consolati et al. [1996], have reported the time dependence of free volume distributions and sizes or shapes of free volume variation from positron annihilation lifetime spectrum experimental data. Although there are some simulated or experimental methods to measure the variances in free volume of gas separation membrane, such as the probe testing method of molecular simulation, the positron annihilation life-time spectroscopy (PALS), or the photochromy method [Verlet, 1967], the free volume morphology is still unknown.

In this study, the effect of tacticity on the fractional free volume, accessible free volume, and free volume morphology in the PMMA membranes was conducted by using molecular simulation and image analysis. By adopting conformation energy minimization and molecular dynamics simulation techniques, various tacticity models of PMMA were constructed and their effects on the accessible free volume, free volume size distribution and morphology were analyzed. Finally, the adsorbed gas on the surface of free volume

†To whom correspondence should be addressed.
E-mail: kuolun@cycu.edu.tw

in s-PMMA was also compared with those in i-PMMA membrane.

THEORETICAL MODELS

The following paragraphs describe the construction methods of the membrane model in detail and also provide a brief description of the molecular dynamics simulation theories for the study of stereo-regular PMMA membrane conformations and their effect on free volume. In the following, the details of the free volume image analysis acquisition for free volume size distribution and morphology employed in this study are described.

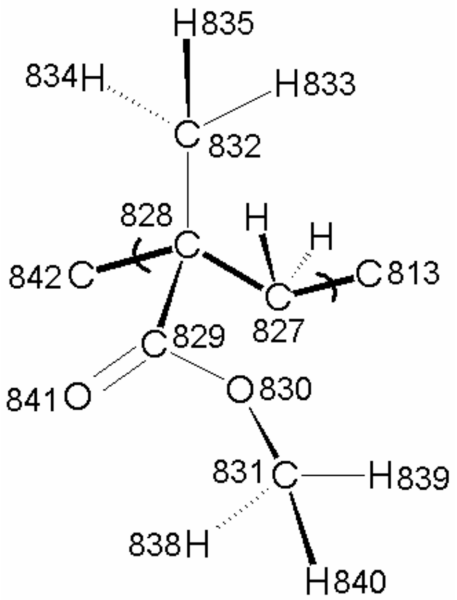

Fig. 1. Monomer unit of PMMA.

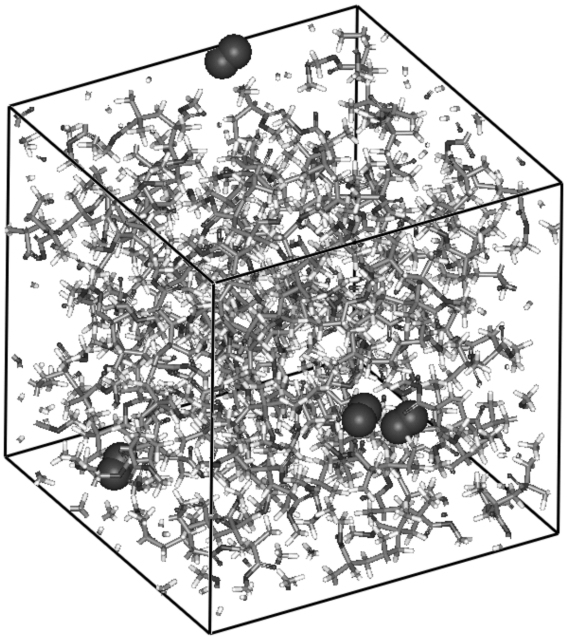

Fig. 2. A schematic diagram of simulating cell with two polymeric chains of s-PMMA and four oxygen molecules in an amorphous cell.

1. Building of the Polymer Matrix

The PMMA monomers were connected to form different stereo-regular tacticity (s/i) as indicated in Fig. 1. The generation of an initial PMMA chain was connected to form different stereo-regular PMMA (the number of C/H/O atoms in cell is 1604/1000/408). In the backbone chain, monomers were connected stepwise by considering proper energy. Two polymer chains and four oxygen molecules were randomly placed into an amorphous cubic cell as shown in Fig. 2 (the amorphous cell parameters: a=b=c=30.3771 Å in s-PMMA, a=b=c=30.0779 Å in i-PMMA), based on self-avoiding walk method. The packing density of polymer cells was defined from the experimental bulk density [Min and Paul, 1988], 1.194 g/cm^3 in s-PMMA and 1.23 g/cm^3 in i-PMMA). During this packing process, the initial distance between polymer and gas molecules was determined by the minimum distance (d_{min}) rule as follow:

$$d_{min}=(r_{vdw,i}+r_{vdw,j})\times(\text{van der Waals scale}), \quad (1)$$

where $r_{vdw,i}$ and $r_{vdw,j}$ are van der Waal's radius of i and j molecules, respectively; and the van der Waals scale is a parameter ranging from 0 to 0.89 (0.3 was chosen in this study). Furthermore, the rotational states of torsion angle were determined from the probability distribution functions, based on energy calculation. For the boundary-effect, three-dimensional periodic boundary conditions (PBC) are also imposed in this amorphous cells system.

The amorphous model and interface region model used in this study are shown in Fig. 3. All atoms in amorphous models were defined by using an *all-atoms* hard sphere model. It included the volume effect of different van der Waals atoms. Five s-PMMA and

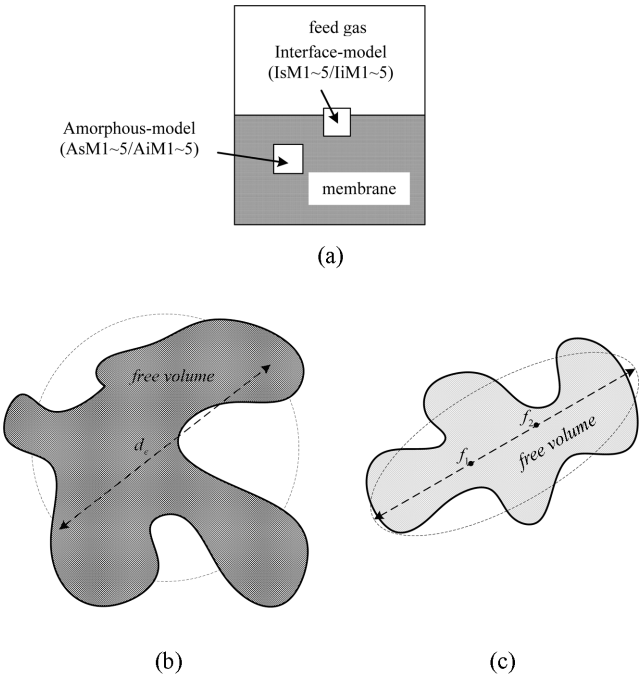

Fig. 3. (a) Definition of amorphous and interface models of stereo-regular PMMA. (b) Calculating free volume size distribution based on equivalent diameter of free volume. (c) Calculating free volume morphology based on free volume and its eccentricity definition in its corresponding ellipse.

five i-PMMA membrane models were built for free volume and accessible free volume image analysis through s-PMMA and i-PMMA membrane by using the Cerius^2 package provided by Accelrys Co. (used to be MSI Co.). All the queuing calculations were performed on the SGI Origin 3000 high performance computer at the National Center for High-Performance Computing (NCHC), ROC. On the other hand, the interface-models were also constructed for adsorbed gas position distribution through two stereo-regular conformations by using Grand Canonical Monte Carlo ensemble method (GCMC) [Allen and Tildesley, 1987; Schlick, 2002].

For the proper local energy minimizing structure, the polymer chain minimization was also utilized in the amorphous cells. The static structure of polymer chains would be determined from the minimum calculating of potential function, calculated by using bonded and non-bonded energy terms in *pcff* (polymer consistent force field) force field [Sun, 1994, 1995; Sun et al., 1994] and applied in PMMA simulation [Soldera and Grohens, 2002; Soldera, 2000, 2002; Lim and Tsotsis, 2003; Subramanian et al., 2001]. The initial structure would be calculated until energy converged or 1000 iterations. By moving randomly one of all atoms in polymer chains, the potential energy of new structure could be calculated and then updated as to give less energy than the previous structure. During the NVT molecular dynamics simulation process, the dynamic motion of polymer atoms in cells was also controlled by *pcff* force field and three-dimensional PBC condition.

The total energy of the *pcff* force field can be classified into three categories: (1) bonded contributions energy terms from each of the polymeric coordinates, (2) cross-effect energy terms between coupled terms from the polymeric coordinates, and (3) non-bonded energy terms, including both van der Waals and an electrostatic force.

$$\begin{aligned}E=&\sum_b[K_2(b-b_0)^2+K_3(b-b_0)^3+K_4(b-b_0)^4]\\&+\sum_\theta[H_2(\theta-\theta_0)^2+H_3(\theta-\theta_0)^3+H_4(\theta-\theta_0)^4]\\&+\sum_\phi\{V_1[1-\cos(\phi-\phi_1^0)]\\&+V_2[1-\cos(2\phi-\phi_2^0)]+V_3[1-\cos(3\phi-\phi_3^0)]\}\\&+\sum_x K_x x^2+\sum_b\sum_{b'}F_{bb'}(b-b_0)(b'-b'_0)+\sum_\theta\sum_{\theta'}F_{\theta\theta'}(\theta-\theta_0)(\theta'-\theta'_0)\\&+\sum_b\sum_\theta F_{b\theta}(b-b_0)(\theta-\theta_0)\\&+\sum_b\sum_\phi(b-b_0)[V_1\cos\phi+V_2\cos2\phi+V_3\cos3\phi]\\&+\sum_{b'}\sum_\phi(b'-b'_0)[V_1\cos\phi+V_2\cos2\phi+V_3\cos3\phi]\\&+\sum_\phi\sum_\theta\sum_{\theta'}K_{\phi\theta\theta'}\cos\phi(\theta-\theta_0)(\theta'-\theta'_0)+\sum_{i>j}\frac{q_iq_j}{\varepsilon r_{ij}}+\sum_{i>j}\left[\frac{A_{ij}}{r_{ij}^9}-\frac{B_{ij}}{r_{ij}^6}\right]\end{aligned}\quad(2)$$

Bonded contribution energy terms consist of 1st covalent bond stretching term, 2nd bond angle bending term and 3rd torsion angle rotation energy terms of the polymer chain. The torsion angle energy is approximately fitted by a Fourier series function. The out-of-plane energy, or 4th improper terms is described as a harmonic function. The cross-interaction terms include the dynamics variation among bond stretching, bending, and torsion angle rotation (5th-10th). The last two terms (11th) and (12th) represent the van der Waals force and Coulombic electrostatic repulsed force. Besides, the van der Waals potential is fitted by *6-9 Lennard-Jones* function rather than *6-12 Lennard-Jones* function for the polymer system.

The energy-minimized conformation of a PMMA polymer can be obtained by calculating the energy terms in the *pcff* force field. The required accuracy was 0.001 kcal/mol, and the non-bonded cut-off distance is 12 Å. Although the minimized stereo-regular conformation was a "local minimum form," it was a more stable structure than other energy forms, which is attributed to the extremely difficult search of a global minimum form.

2. Molecular Dynamics Simulation

The purpose of the dynamic simulation was to calculate the equation of motion for molecules as described by Newton's second law of motion:

$$F_i=m\frac{\partial^2 r_i}{\partial t^2}=-\frac{\partial V}{\partial r_i}. \quad (3)$$

The Verlet basic algorithm [Verlet, 1967] for integration of the equation of Newton's second law of motion is the most widely adopted scheme in molecular dynamics simulation. Modifications to the basic Verlet algorithm have been proposed as the leap frog algorithm [Roe, 1991].

The velocity scale method was widely used in previous molecular dynamics studies [Bruns and Bansal, 1981; Bahar et al., 1993; Chang and Yethiraj, 2001]. The initial velocities of all the atoms were assigned by Maxwell-Boltzmann and Gaussian distribution function.

$$f(v)dv=\left(\frac{m}{2\pi kt}\right)^{3/2}e^{\left(-\frac{mv^2}{2kt}\right)}4\pi v^2dv \quad (4)$$

The velocity components in the coordinate were determined according to the Gaussian distribution equation:

$$g(v_i)dv_i=\left(\frac{m}{2\pi kT}\right)^{1/2}e^{\left(-\frac{mv_i^2}{2kT}\right)}dv_i. \quad (5)$$

and rescaling the velocities until the desired temperature was reached. In this study the velocity and temperature of all atoms were scaled according to

$$\left(\frac{v_{new}}{v_{old}}\right)=\frac{T_{target}}{T_{system}} \quad (6)$$

or by using the rescale factor as

$$\sqrt{\frac{2}{T_K}(T_{target}-T_{system})+1} \quad (7)$$

where T_K is the instaneous kinetic temperature, T_{target} is the target temperature, and T_{system} is the average kinetic temperature.

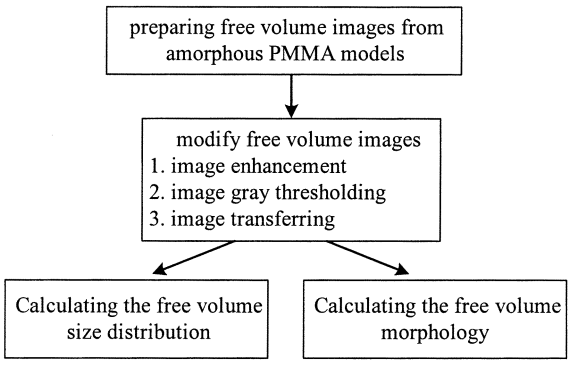

Fig. 4. Flow chart of image analysis in free volume size distribution and morphology of stereo-regular membrane.

3. Image Analysis of the Free Volume

The flow chart of the image analysis method for free volume in separation membrane is indicated in Fig. 4. The cross section images of free volume used in this study are all of equal thickness (1.5 Å). The all free volume images from the membrane models with the size of 256×256 pixels are cleaved at the six different cross-section positions, and at different times (100, 300, 500, 700, 900 ps) from the AsM1-5 and AiM1-5 membrane models.

The following are the steps to analysis the images of free volume.

Step 1: Cleaving the free volume images with RGB colors of the membrane models at different cross-section, such as six cross-section planes at x=0, 0.5; y=0, 0.5, z=0, 0.5.

Step 2: Modifying the images of free volume by using image enhancement (increase the contrast), gray thresholding (choose the threshold to convert a gray-level image) and image transferring (transfer a gray-level image to BW-level image).

Step 3: Based on the BW-level image, analyzing the size distribution and morphology of free volume. The size of free volume is defined by the equivalent diameter of the same area of the circle in BW-level image as indicated in Fig. 3(b). The morphology of free volume is defined by the eccentricity ratio of the corresponding ellipse (eccentricity ratio is the distance between two foci points divided by the major axis length of the corresponding ellipse). Both size distribution and morphology of free volume with pixel units in BW-level image will be transferred to the angstrom units of free volume.

4. Free Volume Analysis by Gas Sorption Simulation

Gas sorption simulation would be realized by construction of PMMA interface models (IsM1-5 and IiM1-5) and use of the Grand Canonical Monte Carlo method (GCMC). For further equilibrium, the velocity scale method was also applied to the initial MD simulation, followed by the 200 ps MD equilibrium simulation. This equilibrium structure was used as an initial sorption model. The cell parameters of interface model are a=b=60.1558 Å (in x/y direction), c=72.754 Å (in z direction), and the PBC was applied. To avoid the interaction of image interface on the top of actual polymer interface in the z direction, the thickness of the polymer membrane and vacuum zone on the top of the interface is 30.3771 and 72.754 Å in the z direction, respectively. The total calculating step number was set 1,000,000, and the sorption sites were determined from the GCMC, based on the calculation of the energy change between the new configuration and the previous configuration.

Gas molecules were randomly placed in a random position and orientation in the interface of stereo-regular membrane models. All the molecules in the interface models were also assumed to follow the atomic interaction function of *pcff* force field. The initial configuration was generated by one of the four moving configurations: create, destroy, translate, and rotate movements of gas molecule.

RESULTS AND DISCUSSION

1. Flexibility of Polymer Chain

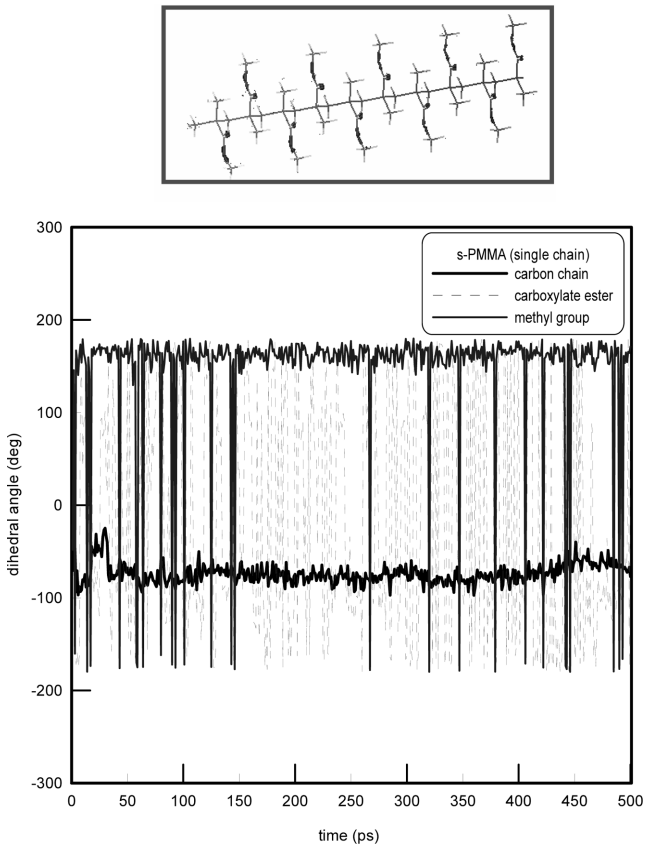

Fig. 5. Dihedral angle dynamics of backbone (carbon chain) and side-chain (carboxylate ester) in s-PMMA membrane (single polymer chain).

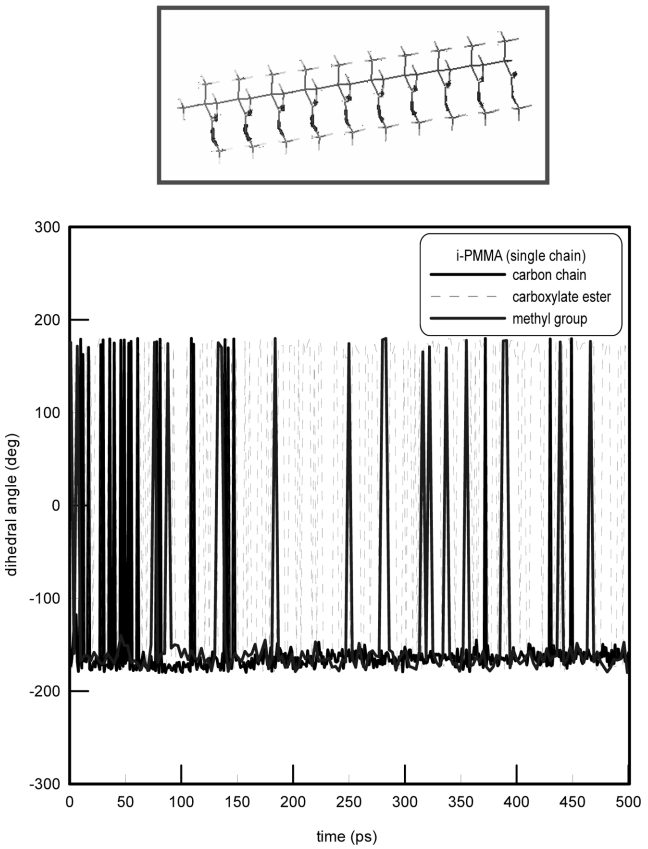

Fig. 6. Dihedral angle dynamics of backbone (carbon chain) and side-chain (carboxylate ester) in i-PMMA membrane (single polymer chain).

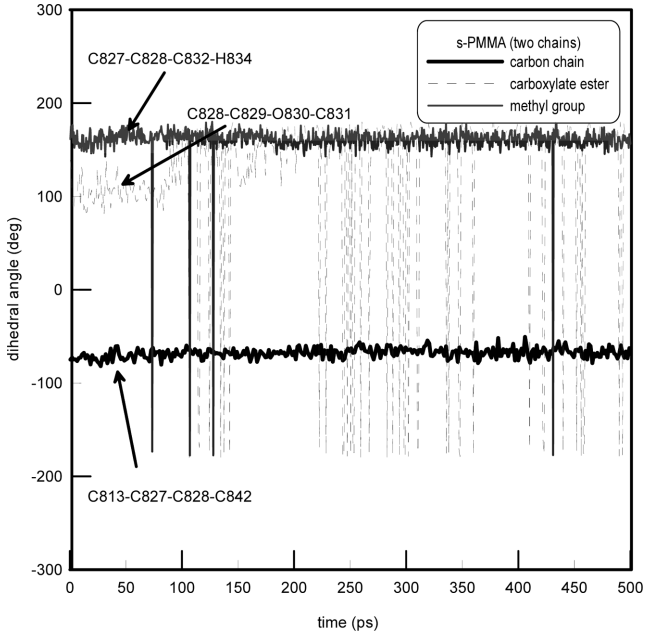

Fig. 7. Dihedral angle dynamics of backbone and side-chain in s-PMMA membrane (two polymer chains).

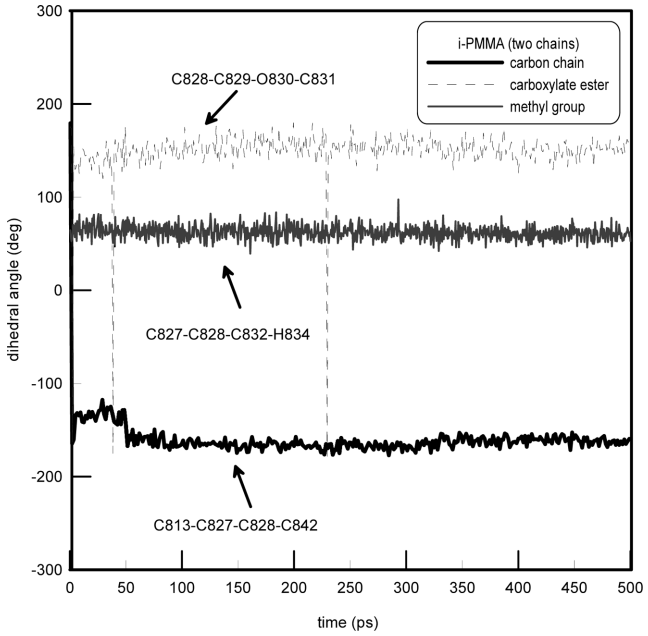

Fig. 8. Dihedral angle dynamics of backbone and side-chain in i-PMMA membrane (two polymer chains).

The dihedral angle dynamics of the backbone (C813-C827-C828-C842) and side chain groups, carboxylate ester group (C828-C829-O830-C831) and methyl group (C828-C832-H834) were calculated to examine the flexibility of the backbone and side chains in PMMA matrices. Figs. 5 and 6 illustrate the comparison of flexibility between backbone and side chain for a single chain condition. Figs. 7 and 8 show the effect of chain interaction on the flexibility of backbone and side chains in a two chain condition. Under the single polymer chain condition, the carboxylate ester group shows a higher mobility than carbon chain, as revealed in both Figs. 5 and 6. This is mainly due to the carboxylate ester group that has a free end while it lacks a backbone in a local viewpoint. The comparison of the flexibility of carboxylate ester group in Figs. 5 and 6 reveals that the carboxylate ester group is more flexible in i-PMMA than in s-PMMA. This discrepancy is caused by the different arrangement of the carboxylate ester group on the carbon chain between i-PMMA and s-PMMA. The stereo orientation of carboxylate ester group on the s-PMMA is one above and one beneath alternatively, while all at the same side on the i-PMMA. As shown in Fig. 5, the dynamic dihedral angles of carboxylate ester group are no more than 150° with respect to the backbone on the s-PMMA chain due to the rotational barriers of the contiguous carboxylate ester groups at the opposite side. However, the carboxylate ester group can rotate in all direction on the i-PMMA chain due to the instability caused by the neighboring carboxylate ester groups. The effect of tacticity on the flexibility of the methyl group is also shown in Figs. 5 and 6. Comparison of these two figures depicts that the methyl group is more flexible in the i-PMMA than that in the s-PMMA. This is also mainly due to the higher stereo barriers of side chain groups in s-PMMA as compared to those in i-PMMA. Allen et al. [1974] studied the rotational barriers of α-methyl group in stereo regular PMMA by NMR and Neutron and reported that the energy of α-methyl dihedral angle barriers is 32 and 23 kJ/mol in s- and i-PMMA, respectively. This means the methyl group side chain is harder to rotate in the s-PMMA than that in the i-PMMA. Comparison of Figs. 5 and 6 also shows that the flexibility of backbones in s-PMMA membrane was smaller than that in i-PMMA. This is also as a result of the higher stereo barriers of the side chain groups in the s-PMMA as compared to those in the i-PMMA; the neighboring side chain at the opposite side suppressed the rotation of the methyl group chain. The lower flexibility of the backbone for the s-PMMA is also supported by the comparison of T_g between the s-PMMA (~118 °C) and the i-PMMA membranes (~35 °C). Furthermore, the more relaxed polymer chain packing density in s-PMMA compared to i-PMMA could be due to the contributions of the intra flexibility of polymer chains. From the comparison of flexibility between the backbone and the sides, it can be concluded that the time course of free volume variation depends considerably on the side chains dynamics than that on the backbone dynamics.

2. Interactions between Polymer Chains

Figs. 6 and 7 reveal the effect of carbon chain interaction on the flexibility of the backbone and the side chains in a double chain system. The dynamics of dihedral angle results proposed that the backbone was almost fixed in a local angle range, while the rotations of the carboxylate ester and the methyl group side chains were more violent in the s-PMMA matrices, as illustrated in Fig. 7. However, comparison of Fig. 7 and Fig. 8 shows quite an interesting phenomenon in that the rotation of the side chains is not so violent in the i-PMMA matrix as compared to that noted in the s-PMMA matrix. This is quite different from that of the single chain condition in which the side chain on an i-PMMA chain showed a more flexible behavior than that on the s-PMMA chain. In the multi-carbon chain system, the stereo barriers are mainly caused by the inter-chain interaction and to a lesser extent by the intra-chain interaction; while in the single carbon chain system, they are caused only by intra-chain interaction. The alternative arrangement of the carboxylate

ester groups in the s-PMMA causes a stronger repulsive interaction between the carbon chains and, thus, enlarges their distance. However, the inter-chain distance in i-PMMA matrix is larger than that in s-PMMA matrix due to the carboxylate ester groups that are located at the same side on the carbon chain and reduces the stereo barrier between carbon chains. In the i-PMMA matrix, there is less space for side chains to rotate; therefore, less flexibility of carboxylate ester groups and methyl groups was observed, as indicated in Fig. 8. Since the diffusion of gas molecules is always in a matrix instead of a polymeric chain system, it can be concluded that due to the lower inter-chain interaction in the s-PMMA matrix, it provides a larger free volume for gas molecules to move through than that in an i-PMMA matrix.

3. Free Volume and Free Volume Morphology

There are two phases in a polymer membrane: a solid phase occupied by polymer chains and a space phase named as free volume. The occupied volume of polymer chains is similar to 1.3 times the van der Waals volume of polymer chains in a separation membrane, and the free volume is the outlines of the van der Waals surface of polymer chains. The well-known definition of fractional free volume (FFV) is defined by specific volume of membrane and occupied volume of polymeric molecules. The FFV was calculated from the formula: $FFV=1-V_0/V_s=1-1.3V_{vdw}/V_s$, where V_s is the specific volume, V_0 is occupied volume of polymer chains and V_{vdw} is van der Waals volume of polymer chains, respectively. In this research, we assumed that the van der Waals volume of polymer is calculated from the volume occupied by van der Waals surface of polymer. The performance of a gas separation membrane usually can be described by solution-diffusion model. The free volume sizes and morphology are very important parameters to the permeability of a separation membrane. Generally speaking, the more fractional free volume of separation membrane, the higher diffusivity or solubility of membrane that will be obtained. However, the defect of the fractional free volume definition is that it is difficult to provide information about free volume morphology and which includes the dead zone volume for actual gas molecules. A comparison of free volume in s-PMMA with that in i-PMMA membrane is illustrated in Figs. 9 and 10 at two different time segments, respectively. The free volume (*i.e.*, gas transfer channel) is wider and longer in s-PMMA matrices, while there is much smaller and closed free volume in i-PMMA according to free volume variation. When gas molecules diffuse in chain networks, there would be a larger transfer phenomenon in the s-PMMA. On the other hand, the free volume cross-section images also indicated the time dependence of sizes or shapes of free volume variation.

4. Mass Distributions

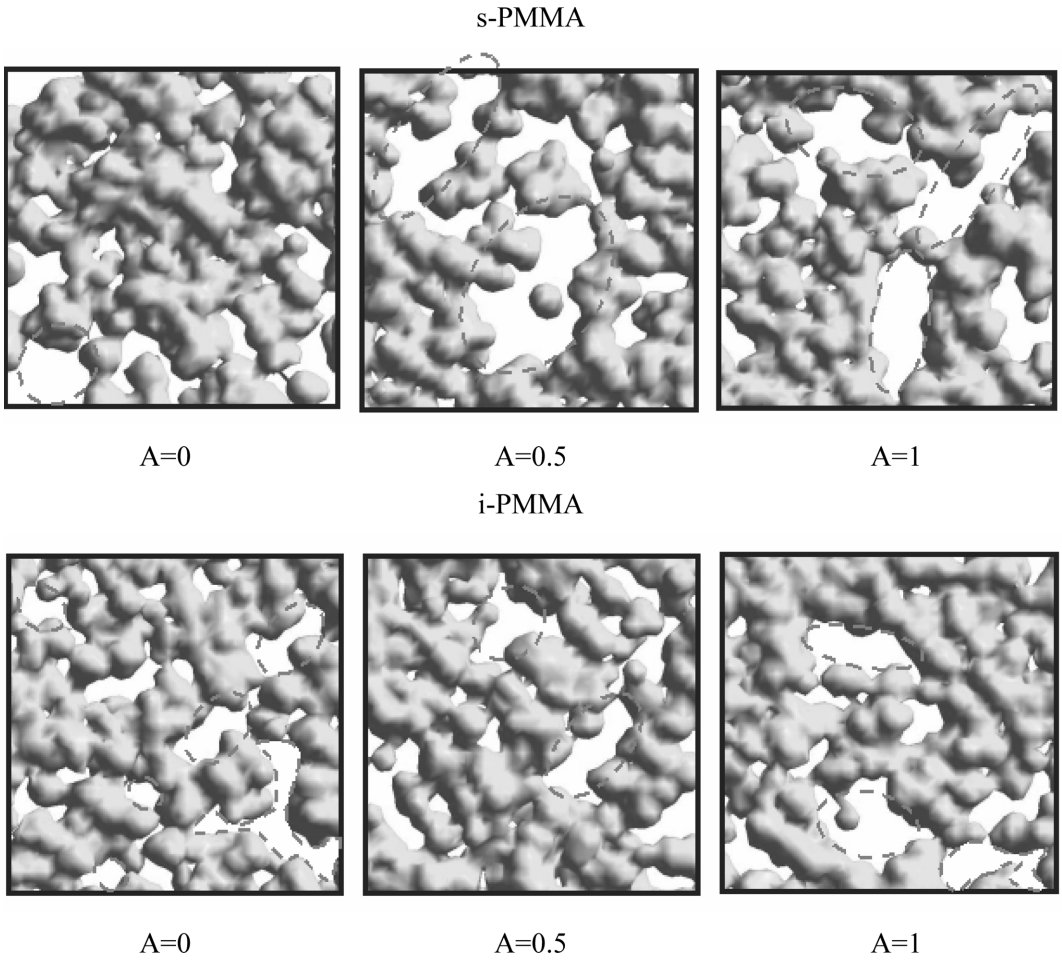

Fig. 9. Free volume variation of s-PMMA(upper)/i-PMMA at 100 ps (A=x/a, a is amorphous cell length, x is free volume cross section position).

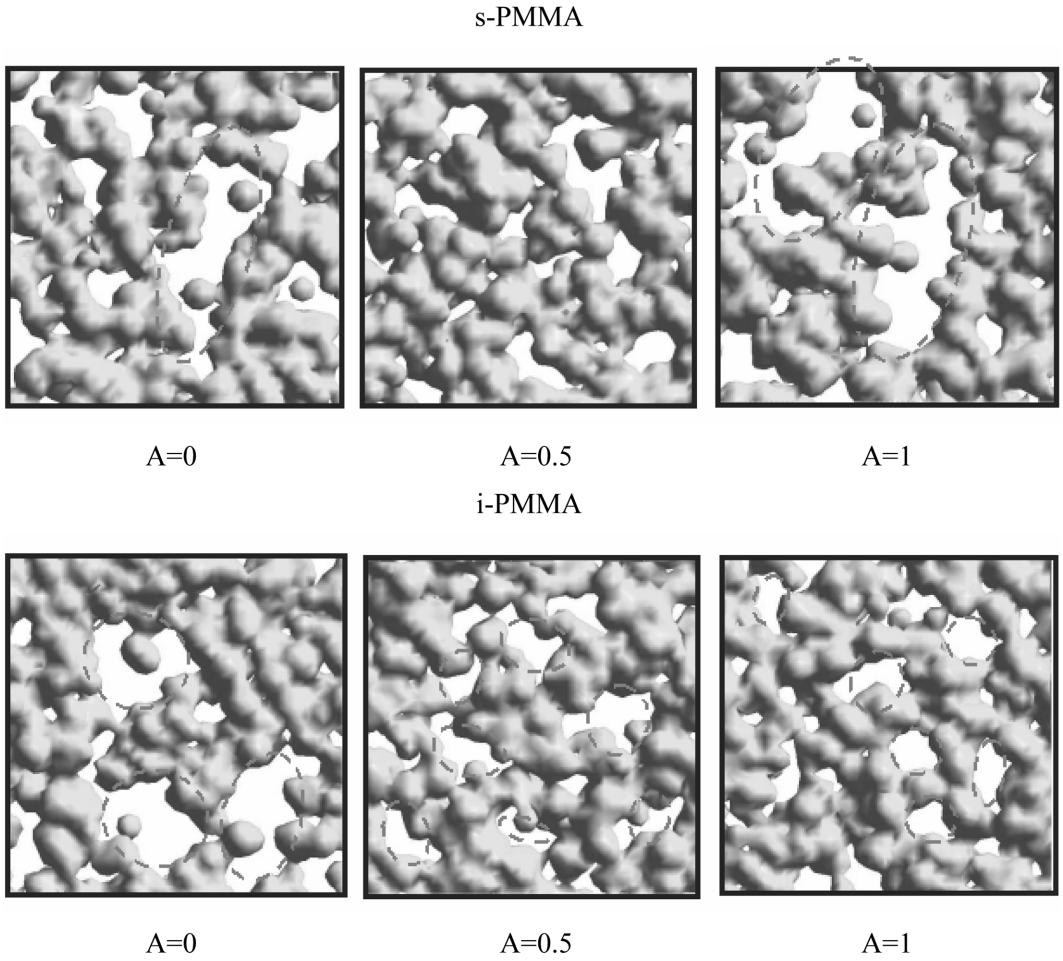

Fig. 10. Free volume variation of s-PMMA(upper)/i-PMMA at 800 ps (A=x/a, a is amorphous cell length, x is free volume cross section position).

The mass distributions of oxygen in AsM1 and AiM1 PMMA models at conditions of temperature of 308 K and 1.5 atm of pressure were simulated by GCMC method as indicated in Fig. 11. The solubility coefficients in stereo-regular PMMA of experimental measurements obtained by Min and Paul [1988] for oxygen in matrix at 308 K temperature and 1-2 atm indicated that the solubility coefficient in s-PMMA is higher than that in i-PMMA membrane (in s-PMMA is 2.61×10^{-3}, i-PMMA is 0.74×10^{-3} cm^3 (STP)/cm^3 cmHg). Obviously, the number of adsorption sites for oxygen in s-PMMA is larger than in i-PMMA matrix. This suggestion is also validated by the mass distributions of oxygen on the projected plane [0,0,1]. The surface of free volume and mass site distribution in s-PMMA are more accessible for oxygen and with more long type free volume in shape. On the other hand, the performance of gas solubility is related with the 3D conformation of polymer chain and free volume morphology of membrane.

5. Interaction Energy

The interaction forces of oxygen sorption in AsM1 and AiM1 PMMA models were only controlled by the non-bonded energy of van der Waals and Coulomb force in the force field. The interaction energy between gas and different stereo-regular polymer frameworks is shown in Fig. 12. The interaction energy of oxygen with s-PMMA (–0.7 kJ/mol) is the same as that with i-PMMA (–0.7 kJ/mod). This is not surprising; the tendency of energy distribution in AsM1-5 is similar to that in Aim1-5 models. When gas is adsorbed on the surface of a membrane, the interaction energy with polymer chains is the same in both s-PMMA and i-PMMA matrix due to the same numbers of carbon, hydrogen, oxygen atoms in methyl methacrylate monomer.

Moreover, according to the thermodynamics theory ($\Delta G=\Delta H-T\Delta S$), the entropy of s-PMMA is higher than that in i-PMMA membrane, which is due to the higher size distribution and more random morphology of free volume. Consequently, in the same enthalpy and higher entropy condition, the gas has a tendency to adsorb on the free volume surface. In order to investigate which one of the van der Waals or Coulomb forces is the major force for gas adsorption in PMMA, we also calculated another stereo-regular model (only controlled by the van der Waals force), and the mass and energy distributions (not shown in here) are also similar to the results, as in Figs. 11 and 12. This means that the most important interaction force for gas adsorption on PMMA is the van der Waals force.

CONCLUSIONS

MD simulation is a powerful tool to study the phenomena in polymer membranes including the membrane morphology and trans-

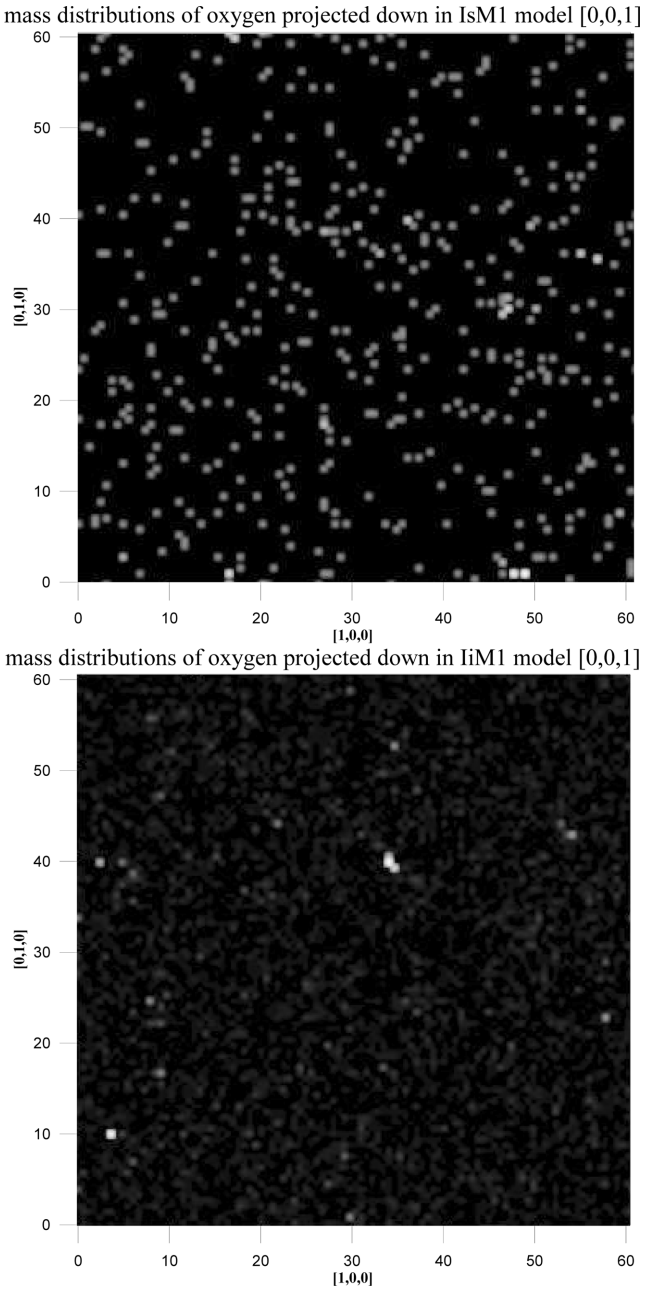

Fig. 11. Mass distributions of oxygen in AsM1 and AiM1 PMMA model (T=308 K, P=1.5 atm).

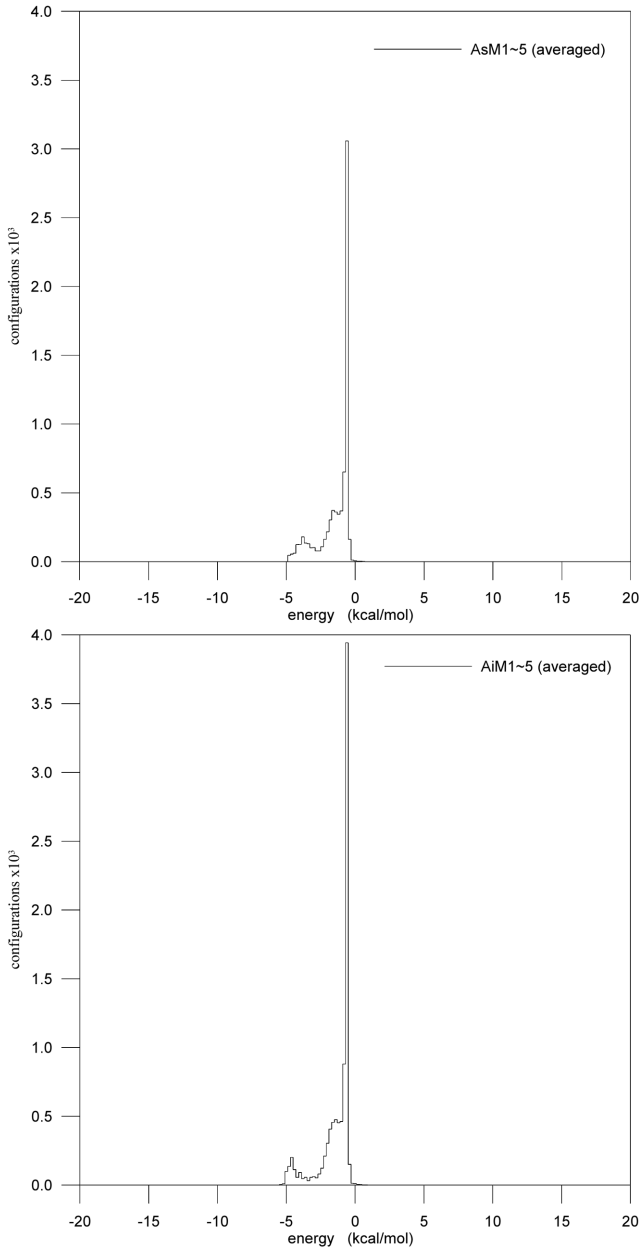

Fig. 12. Energy distributions of oxygen adsorbed configurations in AsM1-5 and AiM1-5 models (T=308 K, P=1.5 atm).

port phenomena through membranes. In this study, the effect of tacticity on the fractional free volume, accessible free volume, and free volume morphology in the PMMA membranes was conducted by using molecular simulation and image analysis. The chain flexibility, chain interaction, end-to-end distance of a chain and the time course of the free volume variation in the various stereo-regular PMMA, were obtained by an MD simulation technique. Simulation results depict that the construction of distinct tacticity has a significant influence on the flexibility of a molecular chain and the morphology of free volume in the syndiotactic (s-) and isotactic (i-) PMMA oligomers. MD calculation of the dynamic microstructure of a PMMA matrix shows that the s-PMMA membrane gives less flexibility in the backbone and a longer end-to-end distance than in the i-PMMA membrane. The less flexibility and longer end-to-end distance in the s-PMMA matrix causes the shapes and sizes of s-PMMA free volume to be longer and larger than those in an i-PMMA membrane. Furthermore, by adopting conformation energy minimization and molecular dynamics simulation techniques, various tacticity models of PMMA were constructed and their effect on the accessible free volume and morphology was analyzed. Results showed that the surface of free volume and sorption site distribution in s-PMMA is more accessible for oxygen due to its long type in shape as compared with those in i-PMMA membrane. Interaction energy analysis reveals that the most important interaction force for gas adsorption on PMMA is the van der Waals force.

ACKNOWLEDGMENTS

The authors wish to express their sincere gratitude to the Ministry of Economic Affairs (MOEA), R.O.C. for the financial support under the grant of the Technology Development Program for Academia (TDPA) project. Computational calculating support from the National Center for High-Performance Computing who provided the SGI O3800 computer and Cerius^2 software is highly appreciated.

NOMENCLATURE

$a_i(t)$: acceleration function of atoms [-]
b : bond length [deg]
b_0 : original bond length [deg]
D_α : self diffusion coefficient of number atoms [cm^2/s]
d_{min} : minimum distance among atoms [Å]
E : potential energy of force field [kJ/mol]
f(v) : Maxwell-Boltzmann distribution function [-]
$g(v_i)$: Gaussian distribution equation [-]
N_α : numbers of diffusion molecule [-]
$r_i(t)$: position function of atoms [-]
θ : bond angle [deg]
θ_0 : original bond angle [deg]
ϕ : torsion angle [deg]
ϕ_0 : original torsion angle [deg]
V : potential energy of force field [kJ/mol]
x : improper torsion angle [deg]

REFERENCES

Allen, G., Wright, C. J. and Higgins, J. S., "Effect of Polymer Microstructure on Methyl Group Torsional Vibrations," *Polymer*, **15**, 319 (1974).

Allen, M. P. and Tildesley, D. J., *Computer Simulation of Liquids*, Clarendon Press, Oxford, 126 (1987).

Bahar, I., Badur, B. and Doruker, P., "Solvent Effect on Translational Diffusivity and Orientational Mobility of Polymers in Solution: A Molecular Dynamics Study," *J. Chem. Phys.*, **99**, 2235 (1993).

Bruns, W. and Bansal, R., "Molecular Dynamics Study of a Single Polymer Chain in Solution," *J. Chem. Phys.*, **74**, 2064 (1981).

Bywater, S. and Toporowski, P. M., "Effect of Stereostructure on Glass Transition Temperatures of PMMA," *Polymer*, **13**, 94 (1972).

Chang, R. and Yethiraj, A., "Solvent Effects on the Collapse Dynamics of Polymers," *J. Chem. Phys.*, **114**, 7688 (2001).

Consolati, G., Genco, I., Pegoraro, M. and Zanderighi, L., "Positron Annihilation Lifetime (PAL) in PTMSP: Free Volume Determination and Time Dependence of Permeability," *J. Polym. Sci., Part B, Polym. Phy.*, **34**, 357 (1996).

Cuperus, F. P., Bargeman, D. and Smolders, C. A., "Permporometry: the Determination of the Size Distribution of Active Pores in UF Membranes," *J. Membr. Sci.*, **71**, 57 (1992).

Dongarra, J., Meuer, H. and Simon, H., "High Performance Computing Today," *AIChE Symposium Series*, **97**, 96 (2001).

Dybal, J., Stokr, J. and Schneider, B., "Vibrational Spectra and Structure of Stereoregular PMMA and of the Stereocomplex," *Polymer*, **24**, 971 (1983).

Goodman, J. M., *Chemical Applications of Molecular Modelling*, Royal Society of Chemistry (1997).

Grohens, Y., Brogly, M., Labbe, C., David, M. O. and Schultz, J., "Glass Transition of Stereoregular PMMA at Interfaces," *Langmuir*, **14**, 2929 (1998).

Hofmann, D., Heuchel, M., Yampolskii, Y., Khotimskii, V. and Shantarovich, V., "Free Volume Distributions in Ultrahigh and Lower Free Volume Polymers: Comparison Between Molecular Modeling and Positron Lifetime Studies," *Macromolecules*, **35**, 2129 (2002).

Koinuma, H., Sato, K. and Hirai, H., "Polymer Conformation and NMR Chemical Shifts, 5[a] ^1H and ^{13}C NMR Spectra of PMMA," *Makromol. Chem.*, **183**, 223 (1982).

Kuebler, S. C., Schaefer, D. J., Boeffel, C. and Spiess, H. W., "2D Exchange NMR Investigation of the α-Relaxation in PEMA as Compared to PMMA," *Macromolecules*, **30**, 6597 (1997).

Lim, S. Y. and Tsotsis, T. T., "Molecular Simulation of Diffusion and Sorption of Gases in an Amorphous Polymer," *J. Chem. Phys.*, **119**, 496 (2003).

MacElroy, J. M. D., "Computer Simulation of Diffusion within and through Membranes using Nonequilibrium Molecular Dynamics," *Korean J. Chem. Eng.*, **17**, 129 (2000).

Mietton-Peuchot, M., Condat, C. and Courtois, T., "Use of Gas-Liquid Porometry Measurements for Selection of Microfiltration Membranes," *J. Membr. Sci.*, **133**, 73 (1997).

Min, K. E. and Paul, D. R., "Effect of Tacticity on Permeation Properties of PMMA," *J. Polym. Sci.*, **26**, 1021 (1988).

Roe, R. J., *Computer Simulation of Polymer*, Englewood Cliffs, NJ, Prentice-Hall, 220 (1991).

Schlick, T., *Molecular Modeling and Simulation*, Springer, New York, 373 (2002).

Schroeder, J. A., Karasz, F. E. and MacKnight, W. J., "Stereoregular PMMAs: Polymer-polymer and Copolymer-polymer Blends," *Polymer*, **26**, 1795 (1985).

Soldera, A. and Grohens, Y., "Local Dynamics of Stereoregular PMMAs Using Molecular Simulation," *Macromolecues*, **35**, 722 (2002).

Soldera, A., "Energetic Analysis of the Two PMMA Chain Tacticities and PMA through Molecular Dynamics Simulations," *Polymer*, **43**, 4269 (2002).

Soldera, A., "Molecular Modeling of Polymer-chain Tacticity," *Polym. Plast. Technol. Eng.*, **39**, 457 (2000).

Subramanian, V., Asirvatham, P. S., Balakrishnan, R. and Ramasami, T., "Molecular Mechanics Studies on Polypropylene and Polymethylmethacrylate Polymers," *Chem. Phys. Lett.*, **342**, 603 (2001).

Sun, H., Mumby, S. J., Maple, J. R. and Hagler, A. T., "An Ab Initio CFF93 All-atom Force Field for Polycarbonates," *J. Am. Chem. Soc.*, **116**, 2987 (1994).

Sun, H., "Ab Initio Calculations and Force Field Development for Computer Simulation of Polysilanes," *Macromolecules*, **28**, 701 (1995).

Sun, H., "Force Field for Computation of Conformational Energies, Structures, and Vibrational Frequencies of Aromatic Polyesters," *J. Comput. Chem.*, **15**, 752 (1994).

Vacatello, M. and Flory, P. J., "Conformational Statistics of PMMA," *Macromolecules*, **19**, 405 (1986).

Verlet, L., "Computer Experiments on Classical Fluids: I Thermodynamical Properties of Lennard-Jones Molecules," *Phys. Rev.*, **159**, 98 (1967).

Vorenkamp, E. J., Bosscher, F. and Challa, G., "Association of Sereoregular PMMA: 4. Further Study on the Composition of the Stereocomplex," *Polymer*, **20**, 59 (1979).